Valence- and conduction-band densities of states for tetrahedral semiconductors: Theory and experiment

J. R. Chelikowsky
Department of Chemical Engineering and Materials Science and Minnesota Supercomputer Institute, University of Minnesota, Minneapolis, Minnesota 55455

T. J. Wagener and J. H. Weaver
Department of Chemical Engineering and Materials Science, University of Minnesota, Minneapolis, Minnesota 55455

A. Jin
Department of Physics, University of Minnesota, Minneapolis, Minnesota 55455
(Received 3 May 1989)

The theoretical and experimental electronic densities of states for both the valence and conduction bands are presented for the tetrahedral semiconductors Si, Ge, GaAs, and ZnSe. The theoretical densities of states were calculated with the empirical pseudopotential method and extend earlier pseudopotential work to 20 eV above the valence-band maximum. X-ray photoemission and inverse-photoemission results make it possible to compare critical-point features in the band structure with experimental structures.

INTRODUCTION

An essential ingredient in determining the electronic properties of solids is the energy distribution of the valence- and conduction-band electrons. For example, analysis of dielectric functions, transport properties, photoemission spectra, and inverse-photoemission spectra for the solid requires knowledge of the electronic density of states. Theoretical quantities such as the total electronic energy of a solid, the position of the Fermi level, and tunneling probabilities of electrons and holes through interfacial barriers call for detailed calculations of the electronic density of states.

Until quite recently, our knowledge of the density of states for semiconductors has emphasized the occupied bands and the first few empty bands. Very successful empirical pseudopotential calculations for tetrahedral semiconductors were based on fitting pseudopotential form factors to measured photoemission and reflectivity spectra.[1] These photoemission spectra supplied direct information about the absolute energies of the valence states, and less direct information about the empty states. Interband transitions from the valence to the lower conduction bands give rise to the reflectivity spectra, and modulation spectroscopy makes it possible to emphasize contributions from particular bands or critical points. Such investigations have led to a high level of confidence for some states, but the reliability of the energy position of the higher conduction bands has been unknown because of incomplete experimental information that could be used to fit the pseudopotential form factors for these bands.

The development of **k**- (or crystal-momentum-) resolved inverse-photoemission spectroscopy (KRIPES) and the application of bremsstrahlung isochromat spectroscopy (BIS) to clean semiconductor surfaces have changed this situation dramatically.[2] Specifically, it is now possible to identify the empty energy levels for the higher conduction bands. In combination with photoemission, inverse photoemission gives a broad overview of *both* occupied and empty states. If this information is combined with reflectivity data, the collection of data provides a stringent test of calculated band structures. In this paper we use such a combined approach to examine tetrahedral semiconductors to test the validity of empirical band structures based on pseudopotential calculations.

We note that *ab initio* methods[3] to understand the optical properties of solids have been developed within the last few years. These new methods include both dynamical screening and local fields in computing the band gaps. They have been able to resolve differences between band gaps calculated within the Hohenberg-Kohn-Sham local-density approximation and those measured experimentally. For example, the measured band gap of Si is reproduced to within a few percent by these new methods, whereas previous theories yielded a band gap which differed from experiment by nearly 50%. [The empirical-pseudpotential-method (EPM) calculations do not have this problem because pseudopotentials are adjusted to fit the measured band gaps.]

While the new theories are very successful in understanding the details of energy bands from first principles, they are too computationally intensive to examine global trends. In contrast, the EPM can be used to calculate energy band structures, densities of states, charge densities, and dielectric response functions using modest personal computers. Moreover, the EPM is easy to implement. The combination of global EPM results and experimental spectra can serve as the standard by which to judge more sophisticated methods.

In this paper we present experimental results for

Si(111), Ge(111), GaAs(110), and ZnSe(100) obtained with x-ray photoemission[1,4] (XPS) and by BIS. We compare these results to the EPM calculations, with emphasis on the high-lying empty states. We note that KRIPES (Ref. 2) and BIS (Ref. 5) studies have been reported for Si, Ge, and GaAs, but no studies have been performed on ZnSe. By examining this set of semiconductors, we gain an overview of how densities of states vary with ionicity trends. Specifically, Ge, GaAs, and ZnSe have the same lattice parameters and the same electronic configuration within the ion core. Hence, differences in electronic structure can be attributed to bonding changes. With the progression from Ge to GaAs to ZnSe, we expect the ionic component of the chemical bond to grow relative to the covalent component.

THEORETICAL TECHNIQUES FOR THE DENSITY OF STATES

The details of the empirical pseudopotential method have been presented elsewhere.[1,6,7] Here, we provide only the essential features. If we use a plane-wave expansion for the basis and potential, then the eigenvalue spectrum of the one-electron Schrödinger equation is given by the solution of the secular equation

$$\det|H(\mathbf{k},\mathbf{G}-\mathbf{G}')-E(\mathbf{k})I|=0\ , \tag{1}$$

where $\mathbf{k}$ is the wave vector, $\mathbf{G}$ is a reciprocal-lattice vector,

$$H(\mathbf{k},\mathbf{G}-\mathbf{G}')=-\left[\frac{\hbar^2k^2}{2m}\right]\delta_{\mathbf{G},\mathbf{G}'}+V(\mathbf{G}-\mathbf{G}')S(\mathbf{G}-\mathbf{G}')\ , \tag{2}$$

$V(\mathbf{G})$ is the pseudopotential form factor, and $S(\mathbf{G})$ is the structure factor. For diamond structures, $S(\mathbf{G})=\cos(\mathbf{G}\cdot\tau)$, where $\tau=2\pi(a,a,a)/8$ and a is the lattice constant. For zinc-blende structures we write $V(\mathbf{G})S(\mathbf{G})$ as $V^s(\mathbf{G})\cos(\mathbf{G}\cdot\tau)+iV^a(\mathbf{G})\sin(\mathbf{G}\cdot\tau)$, where $V^a(\mathbf{G})=[V^C(\mathbf{G})+V^A(\mathbf{G})]/2$ and $V^s(\mathbf{G})=[V^C(\mathbf{G})-V^A(\mathbf{G})]/2$ are the symmetric and antisymmetric form factors, respectively. $V^C(\mathbf{G})$ is the form factor for the cation, while $V^A(\mathbf{G})$ is that for the anion. For spherically symmetric potentials, $V(\mathbf{G})=V(|\mathbf{G}|)$. For the semiconductors of interest here, it is necessary to retain only the form factors $V(G)$, where $G^2=3$, 4, 8, and 11 in units of $(2\pi/a)^2$.

For Si this procedure yields an accurate description of the reflectivity and photoemission spectra.[1] However, for Ge, GaAs, and ZnSe, nonlocal corrections to the pseudopotential are necessary to produce similar accuracy.[7] This is caused by d states within the ion core which modify the conduction-band structure of Ge, GaAs, and ZnSe, and make the pseudopotential nonlocal. This effect cannot be handled by adjusting the form factors in Eq. (2) because they are independent of angular-momentum character. A simple correction for a specific l-dependent term can be written

$$V_{\mathrm{NL}}(\mathbf{k},\mathbf{G}-\mathbf{G}')=V(\mathbf{G}-\mathbf{G}')+4\pi(2l+1)P_l(\cos\theta)\times\int dr\,r^2V_l(r)j_l(Kr)j_l(K'r)/\Omega_a\ , \tag{3}$$

where $\mathbf{K}=\mathbf{k}+\mathbf{G}$, $\cos\theta=\mathbf{K}\cdot\mathbf{K}'/KK'$, Ω_a is the atomic volume, P_l is a Legendre polynomial, j_l is a spherical Bessel function, and $V_l(r)$ is a nonlocal correction to the local potential. $V_l(r)$ is usually taken as a simple form such as a square well or a Gaussian well. Either form results in an analytic form for the matrix elements in Eq. (3). Here, we restrict the nonlocal contributions to d states ($l=2$) and write $V_2(r)=A_2\exp[-(r/R)^2]$. As for the local potential, we can form symmetric and antisymmetric combinations for the nonlocal form factors.

The local pseudopotential form factors for the tetrahedral semiconductors are given in Table I. They are the same as those used earlier in fitting optical and photoemission data.[1] With them, the main photoemission features were produced to within $\sim$0.25 eV, and the main features of the optical spectra to within $\sim$0.1 eV. Note that no direct conduction-band information was used to get these form factors. In this paper we show that they also reproduce our BIS results very well.

With respect to computational details, the energy cutoffs in the matrix in Eq. (1) were determined so that plane waves with $|\mathbf{k}+\mathbf{G}|^2<E_1$ were treated directly; plane waves with $E_1<|\mathbf{k}+\mathbf{G}|^2<E_2$ were treated using Löwdin perturbation theory.[1] We used $E_1\approx8$ Ry and $E_2\approx13$ Ry. For the nonlocal matrix elements, the values of A_2 are given in Table II. R was defined by touching spheres with equal radii for the cation and anion. Since Ge, GaAs, and ZnSe have essentially the same lattice constant, we have used only one value for R, namely $R=2.3$ a.u. Relativistic effects were not considered and spin-orbit interactions have been neglected. Although spin-orbit effects split the states at the top of the valence bands of Ge by 0.3 eV, the effect is less than $\sim$0.1 eV in the conduction bands.[1] This is small compared to our experimental resolution of $\sim$0.7 eV. With the potential fixed by the parameters in Tables I and II, we evaluated

TABLE I. Potential parameters for Eqs. (1) and (2). The form factors are given for G vectors in units of $(2\pi/a)^2$.

	Lattice constant (Å)	Form factors (Ry)					
		Symmetric			Antisymmetric		
	a	$V(3)$	$V(8)$	$V(11)$	$V(3)$	$V(4)$	$V(11)$
Si	5.43	−0.224	0.055	0.072			
Ge	5.65	−0.221	0.019	0.056			
GaAs	5.65	−0.214	0.014	0.067	0.055	0.038	0.001
ZnSe	5.65	−0.218	0.029	0.064	0.139	0.062	0.016

TABLE II. Nonlocal pseudopotential parameters as in Eq. (3).

Element	A_2 (Ry)
Zn	−0.125
Ga	0.125
As	0.625
Se	1.250

$E(\mathbf{k})$ on a grid of ~500 points in an irreducible sector of the first Brillouin zone and determined the density of states by tetrahedral sampling.[8]

It should be noted that the calculated densities of states are not quantitatively comparable to either photoemission or inverse-photoemission spectra unless transition matrix elements are incorporated in the calculations and corrections for inelastic scattering are considered in the experiments. Nonetheless, the primary source of structure in both experiment and theory is from van Hove singularities in the energy-band structure, and matrix-element effects are frequently weak.[1] This is particularly true for XPS (BIS) since final (initial) states are ~1500 eV above the Fermi level. Although matrix elements were not included in the calculated density of states, the effects of experimental resolution and inelastic scattering were simulated by broadening the theoretical structure. Specifically, the density-of-states results were convoluted with a Gaussian with a full width at half maximum of 0.5 eV. Many-body effects have been partly included by adjusting the pseudopotential form factors to agree with the XPS and reflectivity measurements.

EXPERIMENTAL TECHNIQUES

The BIS studies were done in a four-chamber ultrahigh-vacuum system operating at a pressure of 1×10^{-10} Torr.[9] A (1×5)-mm^2 sheet beam of electrons from a Pierce-type electron gun was incident onto the sample at normal incidence. The sample beam current was ~100 μA. A crystal x-ray monochromator was used to select photon energies of 1486.6 eV emitted from the sample. A Chevron channel plate was used to detect those photons. A collected spectrum represents the distribution of unoccupied states. The spectrometer Fermi level was determined from a Pd reference in electrical contact with the sample. Low-energy electron-diffraction (LEED) spectra were measured with reverse-view, four-grid optics. This LEED system was also used for Auger-spectroscopy studies. For the XPS studies we focused a monochromatic beam of Al $K\alpha$ photons onto the surface, and energies of the emitted electrons were measured with a Surface Science Instruments hemispherical analyzer with a resistive-anode, position-sensitive detector. The x-ray-beam size was 300 μm in diameter, and the pass energy of the analyzer was 50 eV. The overall energy resolution is better than 0.7 eV.[10] The XPS experiments were done at 5×10^{-11} Torr.

Well-ordered GaAs(110) surfaces were obtained by cleaving posts of GaAs (Zn doped at 3×10^{18} cm^{-3}). Ge(111) posts were also cleaved *in situ*, and a sharp reconstructed 2×1 LEED pattern was observed. The Sb-doped Ge posts had a resistance of 5–10 Ω cm. Single-crystal p-type Si(111) wafers were sputtered with 500-eV Ar^+ and annealed at 900 °C to get sharp Si(111) 7×7 LEED patterns. n-type ZnSe(100) layers were grown on GaAs(100) substrates in a separate chamber, were Ar^+ sputtered at 600 eV, and were annealed at 400 °C to produce sharp ZnSe(100)-$c(2\times2)$ LEED patterns.[11]

COMPARISON OF THEORY WITH EXPERIMENT

Tables III–VI give the calculated eigenvalues for the lowest 20 bands at points Γ, X, and L for Si, Ge, GaAs, and ZnSe. For simplicity we denote the eigenvalues by symmetry point and energy-band number, e.g., the lowest-energy band at the zone center is written $\Gamma(1)$. The energy zero is the top of the valence band, E_v, or valence-band maximum (VBM). Figures 1–4 show the band structures (bottom panels), the smoothed densities of states (central panels), and the experimental XPS and BIS spectra (top panels). The horizontal axis corresponds to energy, referenced to E_v. Structures in the density of states are labeled with the same notation as in the tables, and the corresponding points in the Brillouin zone follow from inspection of the band structure. The experimental spectra have been normalized for visual clarity and for ease in comparison with the calculations. Note there has been no background subtraction to account for inelastic scattering. Hence, the experimental spectra do not go to zero intensity beneath the valence-band region. Finally, note that the Zn $3d$ core-level emission has been reduced by a factor of 8 for the ZnSe spectra of Fig. 4.

TABLE III. Eigenvalues at high-symmetry points for silicon. The energies are in eV and the valence-band maximum is the zero reference.

Band	$E(\Gamma)$	$E(X)$	$E(L)$
1	−12.64	−8.38	−10.30
2	0	−8.38	−7.38
3	0	−3.08	−1.31
4	0	−3.08	−1.31
5	3.32	1.12	2.03
6	3.32	1.12	3.86
7	3.32	12.18	3.86
8	4.15	12.18	8.67
9	7.09	12.75	11.41
10	7.09	12.75	11.41
11	8.31	13.31	12.66
12	12.49	13.31	12.66
13	12.49	14.95	13.23
14	12.49	14.95	15.13
15	15.61	20.20	21.60
16	27.27	20.20	21.72
17	27.27	20.62	23.42
18	27.27	20.62	23.41
19	28.01	21.50	24.09
20	28.01	21.50	24.09

TABLE IV. Eigenvalues at high-symmetry points for germaniun. The energies are in eV and the valence-band maximum is the zero reference.

Band	$E(\Gamma)$	$E(X)$	$E(L)$
1	−12.63	−8.63	−10.38
2	0	−8.63	−7.59
3	0	−3.25	−1.47
4	0	−3.25	−1.47
5	1.00	1.21	0.81
6	3.24	1.21	4.27
7	3.24	11.64	4.27
8	3.24	11.64	7.19
9	6.01	12.08	10.99
10	8.69	12.08	11.65
11	8.69	12.12	11.65
12	11.27	12.12	11.72
13	11.27	12.81	11.72
14	11.27	12.81	11.97
15	12.87	18.58	18.99
16	25.29	18.58	19.40
17	25.29	18.59	21.49
18	25.29	18.59	21.49
19	26.80	18.85	22.37
20	26.80	18.85	22.37

TABLE VI. Eigenvalues at high-symmetry points for zinc selenide. The energies are in eV and the valence-band maximum is the zero reference.

Band	$E(\Gamma)$	$E(X)$	$E(L)$
1	−12.13	−10.61	−10.97
2	0	−4.86	−4.98
3	0	−1.96	−0.78
4	0	−1.96	−0.78
5	2.89	4.60	4.08
6	7.59	4.85	7.80
7	7.59	13.46	7.80
8	7.59	13.46	9.96
9	9.50	13.50	12.61
10	11.47	13.69	13.64
11	11.47	14.64	13.64
12	13.76	15.64	14.54
13	13.76	15.64	14.87
14	13.76	15.89	14.87
15	16.55	20.49	21.41
16	27.17	20.70	22.69
17	27.17	20.70	23.44
18	27.17	21.41	23.44
19	28.90	21.94	25.03
20	28.90	22.89	25.03

A. Valence-band densities of states

Comparison of Figs. 1 and 2 shows very similar valence bands for Si and Ge. For Ge the experimental and theoretical line shapes in the −6 to −4 eV region are in excellent agreement. The deepest calculated bands appear displaced from experiment, although in a manner opposite to Si, i.e., the Ge bands are ~0.4 eV higher in energy than shown by experiment. Toward the top of the valence band near $L(3,4)$, there appears enhanced emission compared to theory, as for Si.

TABLE V. Eigenvalues at high-symmetry points for gallium arsenide. The energies are in eV and the valence-band maximum is the zero reference.

Band	$E(\Gamma)$	$E(X)$	$E(L)$
1	−12.40	−9.73	−10.50
2	0	−6.76	−6.71
3	0	−2.82	−1.21
4	0	−2.82	−1.21
5	1.65	2.17	1.94
6	4.81	2.51	5.60
7	4.81	12.24	5.60
8	4.81	12.24	7.58
9	6.88	12.51	11.28
10	9.99	12.60	12.49
11	9.99	13.37	12.49
12	12.09	13.37	12.83
13	12.09	13.69	12.90
14	12.09	14.09	12.90
15	12.86	18.85	19.67
16	25.91	19.07	20.37
17	25.91	19.28	22.17
18	25.91	19.28	22.17
19	22.60	19.28	23.32
20	27.60	19.61	23.32

The zinc-blende semiconductors GaAs and ZnSe have valence-band densities of states qualitatively similar to Si and Ge, except for the gap which opens at point X. This gap is related to the different pseudopotentials for the cation and anion potentials. This "antisymmetric" gap has been proposed as a measure of crystal ionicity.[12] It is zero in Si and Ge, but is ~3 eV in GaAs and ~6 eV in ZnSe. The charge density of the lowest valence band from −13 to −10 eV has primarily s character and is localized on the anion. The large peak at −7 to −5 eV comes primarily from the onset of the second valence band at points X and L. The charge density of this band is primarily of cation s character; it changes rapidly to anion p-like at the top of the valence band.

For GaAs the bandwidths and energies are in good agreement with the photoemission results, although the deepest band is predicted to be ~0.5 eV deeper than indicated by experiment. Again, the line shape near the $\Sigma_{\min}$ feature is not well reproduced in experiment, but there is a shoulder in the photoemission spectrum at the predicted energy.

The experimental results for ZnSe (Fig. 4) show very strong emission from the Zn 3d core levels at 8.6 eV relative to the VBM. These 3d states do not interact strongly with the valence bands. This can be seen by examining a series of Zn chalcogenides and noting that the d-band width does not vary from ZnO to ZnTe.[13] Nonetheless, the Zn 3d states may be important in determining the structural properties of Zn compounds, and they could change the details of the valence-band structure.[14] The dominant Zn 3d emission makes it difficult to locate the

valence-band feature predicted at −11 eV. Previous XPS data[4] placed this structure near −14 eV, but our results place it at −12.5 eV. The experimental features at −4.5 and −1.2 eV agree very well with the predictions, although with differences in line shape.

B. Conduction-band densities of states

The conduction bands are more difficult to describe than the valence bands because they are more delocalized and more "free-electron-like" than the valence states. This is particularly true for conduction-band states far removed from the VBM. The free-electron behavior results in more dispersive bands, band crossings, and many van Hove singularities.

Comparison of the results of Figs. 1 and 2 shows that the valence-band structures for Ge and Si are nearly identical, but the conduction bands are not. In particular, the ordering of the first few conduction bands in Si is different from that in Ge or the zinc-blende semiconductors. This difference can be explained by examination of the wave functions for the lowest conduction bands at point Γ and at the Brillouin zone edges, at points L and X. For the lowest conduction band at point Γ, the wave functions exhibit the largest degree of localization and are s-like. At point X or L, however, the states are more free-electron-like.[15,16] A small perturbation of the poten-

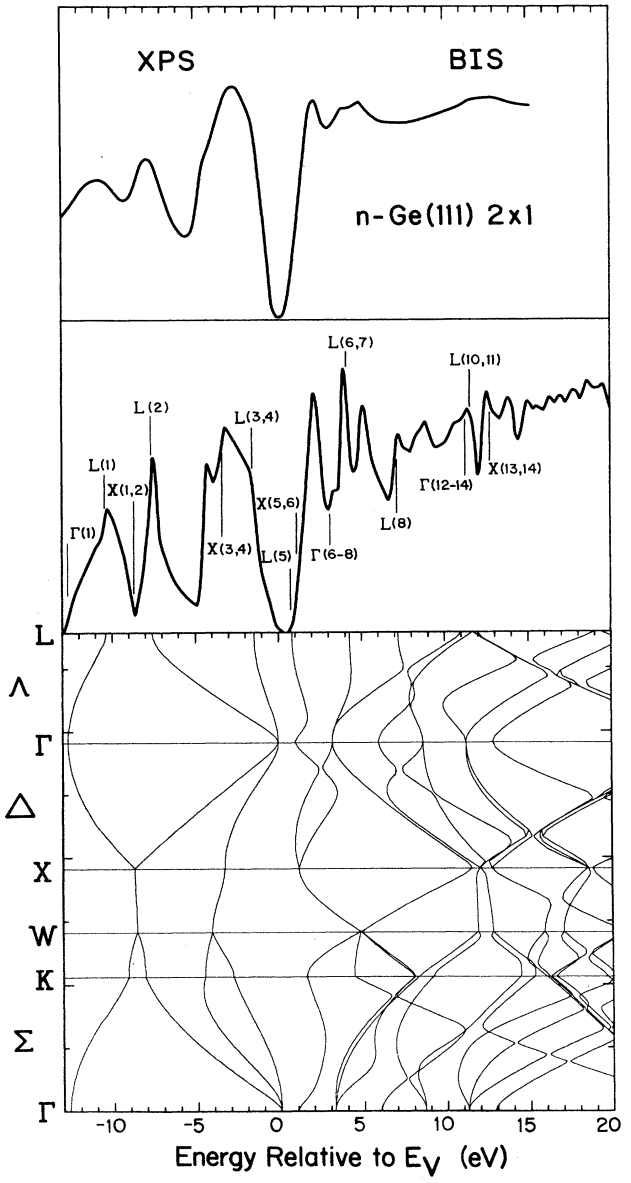

FIG. 1. Calculated energy bands and Gaussian-broadened density of states for silicon compared to experimental XPS and BIS results taken with $h\nu = 1486.6$ eV. The XPS and BIS results are normalized for visual clarity. Experimental backgrounds have not been subtracted.

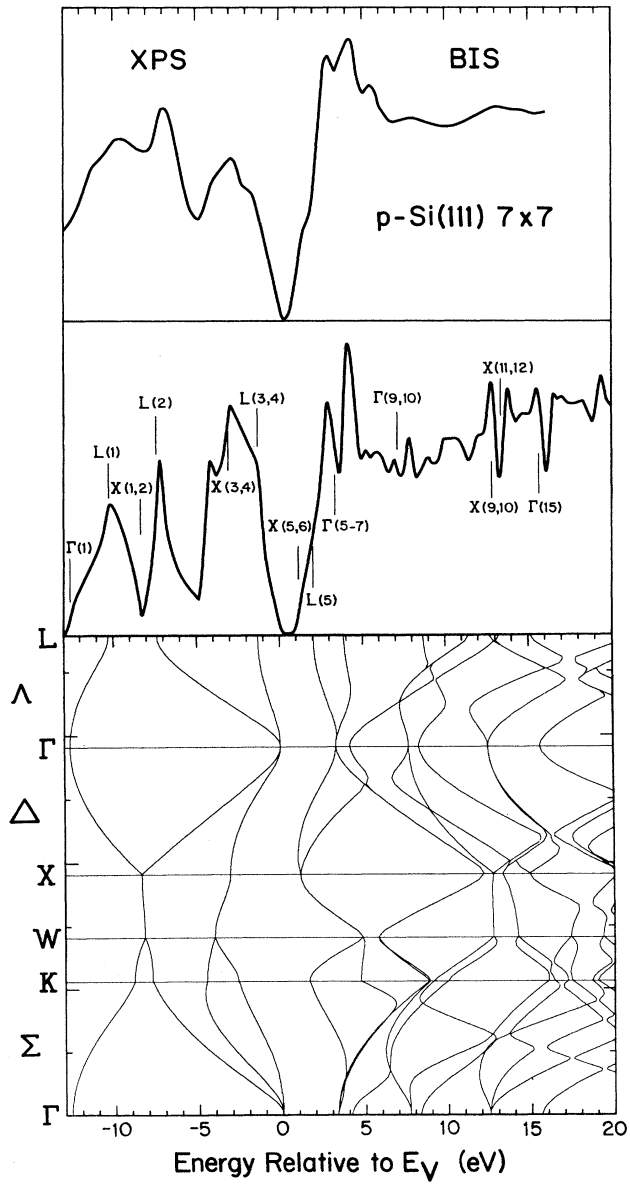

FIG. 2. Calculated and experimental results for germanium, as in Fig. 1.

tial at the atomic site will change the band structure at point Γ more than at point X or L. (Conversely, altering the potential in the interstitial region can affect the bands at point X or L more than at point Γ.)

The conduction-band minimum for Si appears $\sim 80\%$ along the $\Gamma - X$ line.[1] The first two experimental peaks in Si at 2.9 and 4.2 V are in good agreement with theory, and their origin is evident from the calculated band structure near $\Gamma(5-7)$. Structure at 5.5 and 7.5 eV can also be related to the bulk DOS features, but the latter $\Gamma(9,10)$ is broadened, presumably by lifetime effects. The most notable disagreement occurs ~ 10 eV above the VBM, where a peak is predicted but not observed. The predicted structure may arise from the sixth conduction band along L. If so, the placement of this band may be incorrect or the cross section may be small. However, given the free-electron nature of this band, it is unlikely that the inclusion of cross-sections effects would significantly change the peak placement. Finally, a broad feature appears near 13 eV, and this corresponds to calculated structure at $X(,9,10)$ and $X(11,12)$.

The calculated conduction bands for Ge agree with the experiment up to ~ 7 eV. The conduction-band minimum occurs at point L, as is well known, and the first two peaks at 2.2 and 4.0 eV can be identified with the two lowest conduction bands. The peak at 5 eV probably arises from contributions near $W(5-9)$. Although the experimental resolution is not very good in the region above 7 eV because of lifetime broadening, it appears that the gross features are reproduced. The structure from

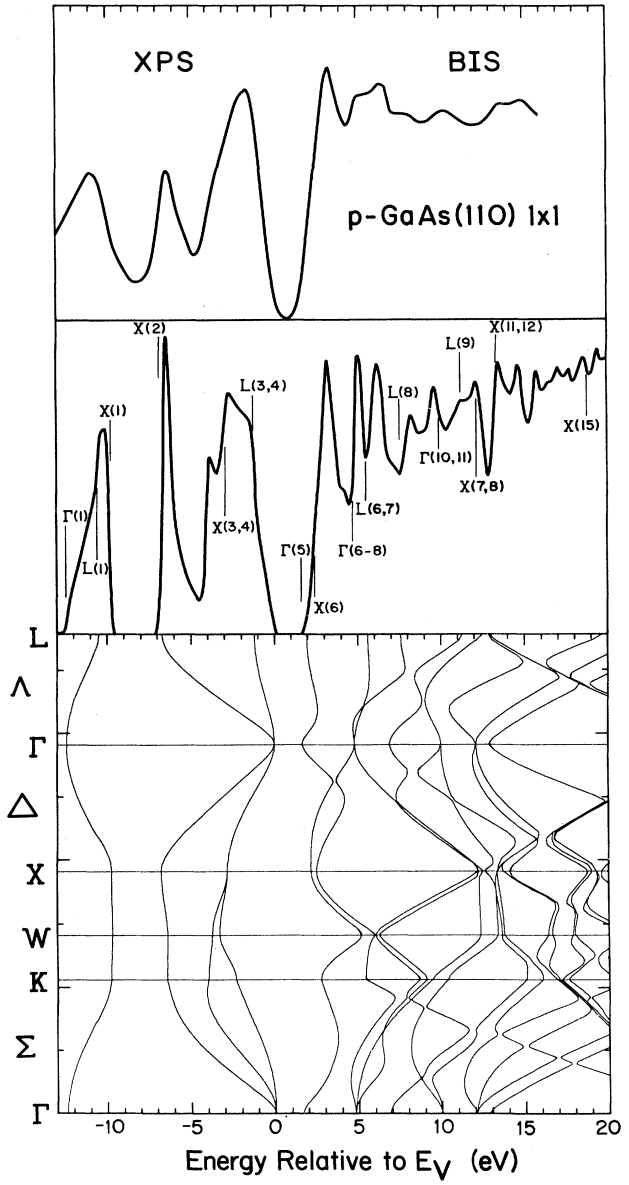

FIG. 3. Calculated and experimental results for gallium arsenide, as in Fig. 1.

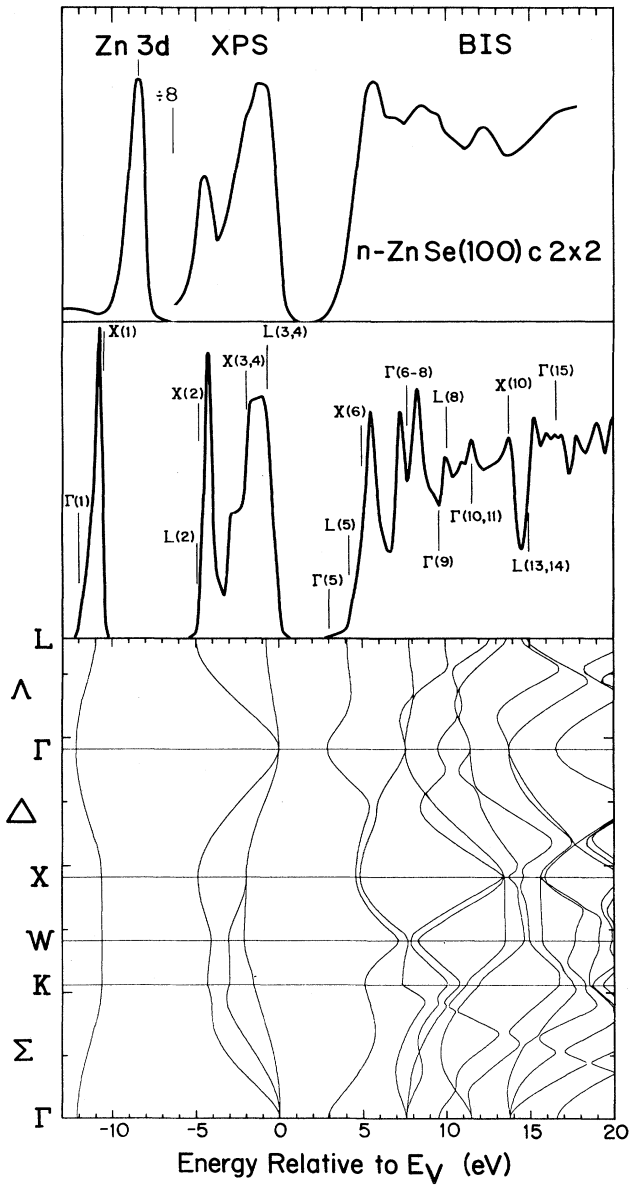

FIG. 4. Calculated and experimental results for zinc selenide, as in Fig. 1.

$L(10,11)$ and from $\Gamma(12-14)$ may cause the broad peak at 11–13 eV.

GaAs is one of the best understood semiconductors, and both the optical spectra and the photoemission spectra have been well reproduced by the EPM.[1,17] GaAs has a direct band gap with the conduction-band minimum at point Γ. Conduction-band structure near 3.3, 5.1, and 6.5 eV is reproduced by theory quite accurately. As for Si and Ge, there is noticeable disagreement between theory and experiment in the region near 10 eV above the VBM. It may be that $X(7,8)$ occurs at a smaller energy than predicted, and this would shift the theoretical structure to lower energies. However, $X(11,12)$ is reproduced in the BIS spectra with the structure at $\sim$15 eV. From the band structure, the latter feature arises from contributions along Δ.

Band structures for ZnSe have been less accurate than those for GaAs when EPM calculations have been compared with experiment. This is not surprising given the presence of the Zn $3d$ core near the valence bands. The general features of the ZnSe conduction bands are similar to those for GaAs in terms of the band ordering and dispersion. Structures at 5.6, 6.8, 8.4, 9.3, and $\sim$10 eV agree with the theoretical density of states, but there seems to be some difficulty in their relative intensities. For example, the two experimental structures at 8.4 and 9.3 eV correspond more closely in intensity to those calculated at 7.2 and 8.2 eV. However, their positions overlap with the strong 8.2-eV feature and the weak 9.1-eV feature. These intensity differences are surprising since they do not exist between the VBM and 7 eV for the other semiconductors. At higher energies there are significant differences. Specifically, the BIS features from 10 to 14 eV above the valence band appear in only qualitative agreement with theory. It is probable that the EPM places the $X(10)$ band too high in energy by about 1 eV.

Finally, we note the great similarity in the conduction-band density of states for the series Ge to GaAs to ZnSe. The main features of the conduction-band densities of states are not changed by the increasing ionicity of the crystals. This is not true for the valence-band densities of states, and there is no real analog in the conduction bands for the antisymmetric gap in the valence bands. The largest effect of increasing ionicity is to increase the band gaps from Ge to GaAs to ZnSe, but not to change significantly the band dispersion. Considering the free-electron-like behavior of the conduction bands, this similarity is not surprising.

CONCLUSIONS

Our results have shown that empirical pseudopotential calculations yield accurate densities of states for the valence bands and for the first several conduction bands. Indeed, the predicted EPM features agree with XPS and BIS spectra to within about 0.5 eV from the bottom of the valence band to $\sim$10 eV above the VBM. Above 10 eV the large number of bands and the fact that the BIS results are broader and may be derived from several features makes it difficult to determine unequivocally whether the EPM is in error. This conclusion of good experimental and theoretical agreement differs from early comparisons between EPM and photoemission spectra. In that EPM work the pseudopotentials were fitted only to optical data and, when the band structures were compared to photoemission spectra, the results were far from satisfactory.[1] Here, the nonlocal pseudopotentials include explicit $l=2$ contributions, and they reproduce photoemission and reflectivity data. Thus, it is reassuring that the extended results agree with experiment.

ACKNOWLEDGMENTS

These studies were supported by the U.S. National Science Foundation under Grant No. DMR-86-10837. The authors wish to thank D. M. Hill, H. M. Meyer, III, M. Vos, and F. Xu for contributing the XPS spectra. One of us (J.R.C.) would like to thank the Minnesota Supercomputer Institute for a grant of computational support.

[1]See, for example, M. L. Cohen and J. R. Chelikowsky, *Electronic Structure and Optical Properties of Solids* (Springer-Verlag, New York, 1988).

[2]For BIS, see C. C. Chu and P. E. Best, Phys. Rev. B **12**, 4575 (1975); **19**, 3414 (1979); H. J. W. M. Hoekstra, W. Speier, R. Zaller, and J. C. Fuggle, *ibid.* **34**, 5177 (1986). For KRIPES, see D. Straub, M. Skibowski, and F. J. Himpsel, Phys. Rev. B **32**, 5237 (1985); D. Straub, L. Ley, and F. J. Himpsel, *ibid.* **33**, 2607 (1986).

[3]M. S. Hybertsen and S. G. Louie, Phys. Rev. B **34**, 5390 (1986), and references therein.

[4]L. Ley, S. Kowalcyzk, R. Pollak, and D. Shirley, Phys. Rev. Lett. **29**, 1088 (1972); L. Ley, R. Pollak, F. R. McFeely, S. Kowalcyzk, and D. Shirley, Phys. Rev. B **9**, 600 (1974), and references therein. See also Ref. 1

[5]H. W. J. M. Hoekstra, W. Spier, R. Zaller, and J. C. Fuggle, Phys. Rev. B **34**, 5177 (1986); W. B. Jackson and J. W. Allen, *ibid.* **37**, 4618 (1988).

[6]J. R. Chelikowsky, D. J. Chadi, and M. L. Cohen, Phys. Rev. B **8**, 2786 (1973).

[7]J. R. Chelikowsky and M. L. Cohen, Phys. Rev. B **14**, 556 (1976).

[8]G. Lehmann and M. Taut, Phys. Status Solidi B **54**, 469 (1972).

[9]Y. Gao, M. Grioni, B. Smandek, J. H. Weaver, and T. Tyrie, J. Phys. E **21**, 488 (1988).

[10]S. A. Chambers, D. M. Hill, F. Xu, and J. H. Weaver, Phys. Rev. B **35**, 634 (1987).

[11]J. M. DePuydt, H. Cheng, J. E. Potts, T. L. Smith, and S. K. Mohapatra, J. Appl. Phys. **62**, 4756 (1987).

[12]A. Wall, Y. Gao, A. Raisanen, A. Franciosi, and J. R. Chelikowsky (unpublished).

[13]D. J. Chadi, W. D. Grobman, and M. L. Cohen, Phys. Rev. B **8**, 5587 (1973).

[14]R. A. Powell, W. E. Spicer, and J. C. McMenamin, Phys. Rev.

B **6**, 3056 (1972); J. R. Chelikowsky, Solid State Commun. **22**, 351 (1971), and references therein.
[15]J. R. Chelikowsky, Phys. Rev. B **35**, 1174 (1987).
[16]H. W. A. M. Rompa, M. F. H. Schuurmans, and F. Williams, Phys. Rev. Lett. **52**, 675 (1984).
[17]S. Richardson, S. G. Louie, M. L. Cohen, and J. R. Chelikowsky, Phys. Rev. B **33**, 1177 (1986).
[18]D. E. Aspnes, C. G. Olson, and D. W. Lynch, Phys. Rev. Lett. **37**, 766 (1976).